DP-MS-81-125

FLOW LINES AND MICROSCOPIC ELEMENTAL INHOMOGENEITIES IN AUSTENITIC STAINLESS STEELS

by

W. Clanton Mosley, Jr.

E. I. du Pont de Nemours & Company
Savannah River Laboratory
Aiken, South Carolina 29808

A Paper Proposed for Presentation at the
16th Annual Meeting of the
Microbeam Analysis Society
Washington, DC
August 9-13, 1982
and for Publication in the Proceedings

This paper was prepared in connection with work done under Contract No. DE-AC09-76SR00001 with the U.S. Department of Energy.

DP-MS-81-125

FLOW LINES AND MICROSCOPIC ELEMENTAL INHOMOGENEITIES IN AUSTENITIC STAINLESS STEELS

W. C. Mosley, Jr.

Flow lines in mechanically formed austenitic stainless steels are known to influence fracture behavior.[1] Enhancement of flow lines by chemical etching is evidence of elemental inhomogeneity. This paper presents the results of electron microprobe analyses to determine the nature of flow lines in three austenitic stainless steels: 21Cr-6Ni-9Mn, 304L, and 19Ni-18Cr.

Experimental

Each stainless steel specimen was prepared for metallographic examination by grinding, polishing and chemical etching. Areas to be analyzed were marked with hardness indentations and photographed. Specimens were then repolished leaving the indentations to help relocate the analysis areas. An Applied Research Laboratories Scanning Electron Microprobe Quantometer (SEMQ) was used to automatically analyze about fifty equally-spaced points along lines perpendicular to the flow lines. Each point was analyzed for Cr, Mn, Fe, Ni, P, S, Al, and Si. X-ray intensities of the four major elements were measured with the same spectrometer. Standards were National Bureau of Standards standard reference materials, pure metals, and well-characterized simple compounds. X-ray intensities

---

W. C. Mosley is employed by E. I. du Pont de Nemours and Co., Savannah River Laboratory, Aiken, SC.

were converted to elemental concentrations with an online version of Magic IV.[2] Each analysis required about ten minutes; therefore, data for each point were normalized to compensate for instrumental drift. Analysis precision was determined by performing ten analyses of a single point on a reference specimen of each steel. After analysis, specimens were again etched and photographed to correlate the flow lines with the analysis points which were marked by spots caused by the electron beam. Elemental concentrations for the points along each analysis line were averaged to yield a bulk composition. Standard deviations and ranges in the elemental concentrations are measures of inhomogeneity. Results are also presented as elemental concentration profiles, correlations between concentrations of alloying elements and the concentration of iron, and histograms showing the distributions of elemental concentrations.

Flow lines were observed in specimens of 21Cr-6Ni-9Mn stainless steel from hot rolled bar, a hot cross rolled plate and high energy rate forgings (seven forging steps) made from the plate. Locations of flow lines correlate with areas depleted in manganese, nickel and, possibly, chromium (chromium inhomogeneity is only slightly greater than the analysis precision). Elemental concentration profiles across flow lines on the specimen from the seventh step of high energy rate forging (Figure 1) are shown in Figure 2. Concentrations of the major alloying elements decrease

with increasing iron concentration as shown in Figure 3 and are described by:

$$Cr(wt\ \%) = 20.73 - 0.036 \times Fe(wt\ \%),$$

$$Mn(wt\ \%) = 34.52 - 0.386 \times Fe(wt\ \%) \text{ and}$$

$$Ni(wt\ \%) = 41.31 - 0.530 \times Fe(wt\ \%)$$

for $62.5 \leq Fe(wt\ \%) \leq 66.5$.

Results for the bar and plate specimens showed essentially the same correlations between elemental concentrations. Elemental inhomogeneities in the specimens from the first and seventh steps of high energy rate forging are the same and are greater than those in the bar and plate (Table 1). The histogram in Figure 4 shows narrow, symmetrical elemental concentration distributions for the plate specimen while those for the high energy rate forging are broader with the iron distribution having a skewness towards lower concentrations.

Flow lines were observed in specimens of 304L stainless steel from hot rolled bar and a high energy rate forging but not in a specimen from hot cross rolled plate. Also, ferrite was present as stringers in the plate and forging. In the forging, the stringers and flow lines were parallel. SEMQ results are presented in Table 2 and Figures 5-8. Locations of flow lines occur in areas enriched in chromium and iron and depleted in nickel and, possibly, manganese (manganese inhomogeneity is only slightly greater than the analysis precision). Elemental concentration correlations for the austenite in the high energy rate forging are described by:

$$Cr(wt\ \%) = -10.17 + 0.394 \times Fe(wt\ \%),$$

$$Ni(wt\ \%) = 98.65 - 1.257 \times Fe(wt\ \%) \text{ and}$$

$$Mn(wt\ \%) = 7.64 - 0.086 \times Fe(wt\ \%)$$

for $68.8 \leq Fe(wt\ \%) \leq 71.2$. Elemental inhomogeneities in the austenite are significantly lower for the plate than for the forging which probably accounts for the absence of flow lines. Chromium and iron concentrations are symmetrically distributed for the plate specimen while the nickel distribution is slightly skewed towards higher concentrations. Elemental concentration distributions for the high energy rate forging are broader with those for iron and chromium being skewed towards lower concentrations.

Analysis of a specimen from a forging of 19Ni-18Cr stainless steel (Figures 9 and 10) showed that flow lines occur in areas enriched in nickel and chromium. A specimen of the casting from which the forging was made was also analyzed (Figures 11 and 12). The dendritic cell boundaries of the casting were also enriched in nickel and chromium. Elemental inhomogeneities in the forging were slightly less than those in the casting (Table 3). Elemental concentration correlations are described by:

$$Cr(wt\ \%) = 57.33 - 0.635 \times Fe(wt\ \%) \text{ and}$$

$$Ni(wt\ \%) = 43.13 - 0.375 \times Fe(wt\ \%)$$

for the forging (Figure 13), and

$$Cr(wt\ \%) = 55.51 - 0.613 \times Fe(wt\ \%) \text{ and}$$

$$Ni(wt\ \%) = 46.86 - 0.428 \times Fe(wt\ \%)$$

for the casting for $61.4 \leq Fe(wt\ \%) < 65.6$. The forging and casting had similar elemental concentration distributions which are skewed towards low iron concentrations and high nickel and chromium concentrations (Figure 14).

Conclusions

Flow lines in mechanically formed austenitic stainless steels correlate with elemental inhomogeneities. Areas in which flow lines occur correspond to austenite compositions that are the last to solidify during cooling from the melts. These inhomogeneities are given directionality by the forming processes. Results for the 304L stainless steel hot cross rolled plate indicate that homogenization can prevent flow line formation. However, high energy rate forging of 304L and 21Cr-6Ni-9Mn stainless steels appears to have increased elemental inhomogeneity and enhanced the flow lines. It is unusual that a mechanical process could cause such a chemical change.

Acknowledgements

The author thanks C. L. Angerman and G. R. Caskey of the Savannah River Laboratory for furnishing the steel specimens.

The information contained in this article was developed during the course of work under Contract No. DE-AC09-76SR00001 with the U.S. Department of Energy.

References

1. M. R. Dietrich et al., "J-Controlled Crack Growth As An Indicator of Hydrogen-Stainless Steel Compatibility," in I. M. Bernstein and Anthony W. Thompson, Ed., Hydrogen Effects in Metals, The Metallurgical Society of AIME, 1981, 637-643.

2. W. J. Hamilton et al., "Automated Electron Microprobe Analysis: A System for the ARL-SEMQ Based on Mass Storage and Speed Capabilities of the Flexible-Magnetic Disk," Microbeam Analysis--1977, 52A.

TABLE 1.--SEMQ analyses of 21Cr-6Ni-9Mn steel specimens.[1]

Element[2]		Point on annealed specimen	Hot rolled bar	Hot cross rolled plate	High energy rate forging	
					1st step	7th step
Cr	Max.	19.08	19.55	18.45	18.91	18.82
	Avg.	18.82	18.90	18.05	18.36	18.41
	Min.	18.65	18.54	17.73	17.75	17.90
	Std.dev.	0.15	0.20	0.17	0.24	0.20
	Range	0.43	1.01	0.72	1.16	0.92
Mn	Max.	9.37	10.46	10.07	10.25	10.51
	Avg.	9.26	9.74	9.63	9.44	9.49
	Min.	9.22	9.24	9.22	8.81	8.75
	Std.dev.	0.06	0.25	0.21	0.38	0.35
	Range	0.15	1.22	0.86	1.44	1.76
Fe	Max.	64.32	64.29	66.32	66.69	66.48
	Avg.	64.03	63.11	65.18	64.94	64.76
	Min.	63.75	61.08	64.12	62.85	62.48
	Std.dev.	0.16	0.58	0.55	0.93	0.85
	Range	0.57	3.21	2.20	3.84	4.00
Ni	Max.	7.26	8.46	7.52	7.96	8.02
	Avg.	7.09	7.60	6.94	6.98	7.02
	Min.	6.93	6.85	6.39	6.00	5.98
	Std.dev.	0.10	0.38	0.29	0.49	0.49
	Range	0.33	1.61	1.13	1.96	2.04
Si	Max.	0.68	0.40	0.21	0.26	0.24
	Avg.	0.65	0.36	0.18	0.19	0.19
	Min.	0.59	0.31	0.16	0.13	0.16
	Std.dev.	0.03	0.02	0.01	0.03	0.02
	Range	0.09	0.09	0.05	0.13	0.08

1) Results in wt %.

2) Al, S, and P below detection limits of ~0.1 wt %.

TABLE 2.--SEMQ analyses of 304L steel specimens.[1]

Element[2]		Point on high energy rate forging	Hot rolled bar	Hot cross-rolled plate[3]		High energy rate forging[4]
				Austenite	Ferrite	Austenite
Cr	Max.	17.56	18.14	18.75	26.08	18.08
	Avg.	17.32	17.37	17.95	25.38	17.46
	Min.	17.14	16.75	17.34	24.69	16.63
	Std.dev.	0.13	0.30	0.30	0.65	0.46
	Range	0.42	1.39	1.41	1.39	1.45
Mn	Max.	1.64	2.07	1.51	1.32	1.71
	Avg.	1.56	1.88	1.44	1.27	1.59
	Min.	1.51	1.72	1.35	1.24	1.45
	Std.dev.	0.03	0.09	0.03	0.03	0.06
	Range	0.13	0.35	0.16	0.08	0.26
Fe	Max.	70.92	68.49	70.30	68.27	71.19
	Avg.	70.73	67.25	69.57	67.92	70.20
	Min.	70.35	65.75	68.85	67.45	68.75
	Std.dev.	0.22	0.75	0.32	0.37	0.56
	Range	0.57	2.74	1.45	0.82	2.44
Ni	Max.	10.42	14.13	11.51	5.12	12.08
	Avg.	10.00	12.82	10.38	4.68	10.43
	Min.	9.73	11.12	9.51	4.37	9.79
	Std.dev.	0.19	0.88	0.48	0.32	0.78
	Range	0.69	3.01	2.00	0.75	2.29
Si	Max.	0.29	0.63	0.51	0.58	0.30
	Avg.	0.25	0.57	0.47	0.54	0.23
	Min.	0.21	0.51	0.43	0.51	0.10
	Std.dev.	0.02	0.03	0.02	0.03	0.06
	Range	0.08	0.12	0.08	0.07	0.20

1) Results in wt %.

2) Al, S, and P below detection limits of $\sim$0.1 wt %.

3) No flow lines observed.

4) Ferrite stringers too thin to analyze.

TABLE 3.--SEMQ analyses of 19Ni-18Cr steel specimens.[1]

Element[2]		Point on forging	Casting	Forging
Cr	Max.	15.90	18.20	18.26
	Avg.	15.76	16.47	16.48
	Min.	15.63	15.42	15.64
	Std.dev.	0.10	0.70	0.63
	Range	0.27	2.78	2.62
Fe	Max.	63.12	65.28	65.58
	Avg.	63.00	63.68	64.37
	Min.	62.80	60.82	61.40
	Std.dev.	0.11	1.12	1.01
	Range	0.32	4.46	4.18
Ni	Max.	21.27	20.65	20.25
	Avg.	21.05	19.63	18.96
	Min.	20.87	18.91	18.35
	Std.dev.	0.10	0.47	0.42
	Range	0.40	1.74	1.90

1) Results in wt %.

2) Mn, Al, Si, P, and S less than detection limits of ∿0.1 wt %.

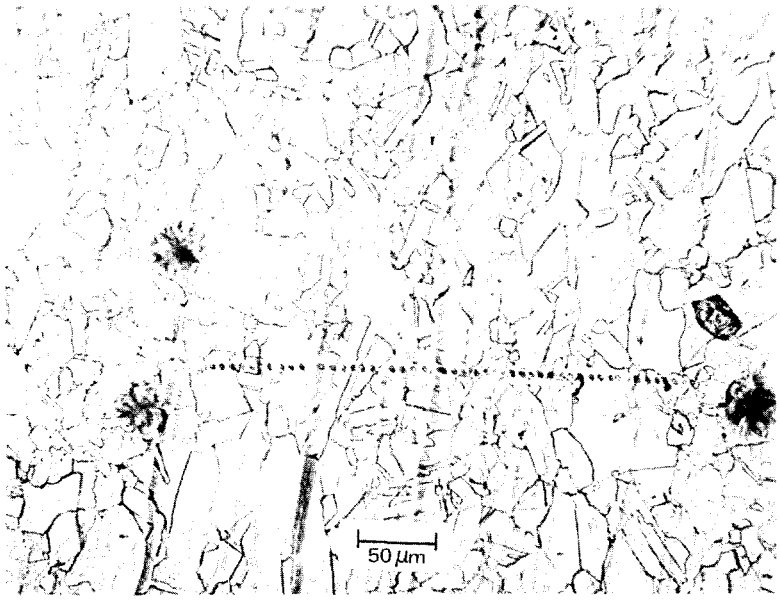

FIG. 1.--High energy rate forged 21Cr-6Ni-9Mn stainless steel.

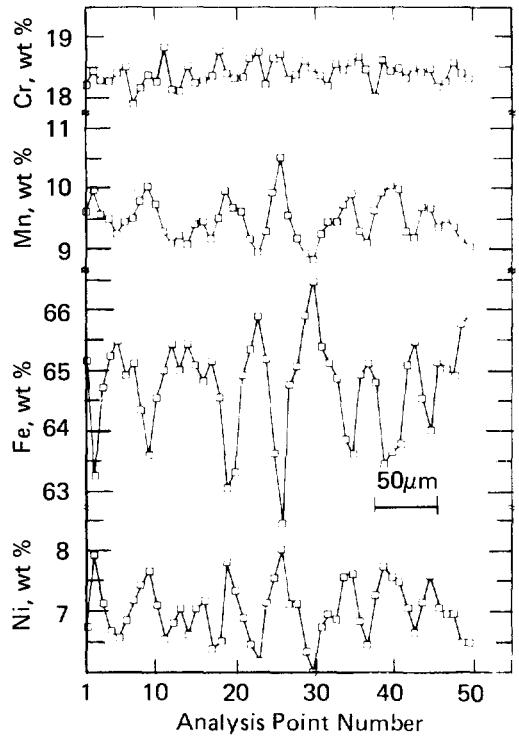

FIG. 2.--Elemental concentration profiles across flow lines in high energy rate forged 21Cr-6Ni-9Mn stainless steel.

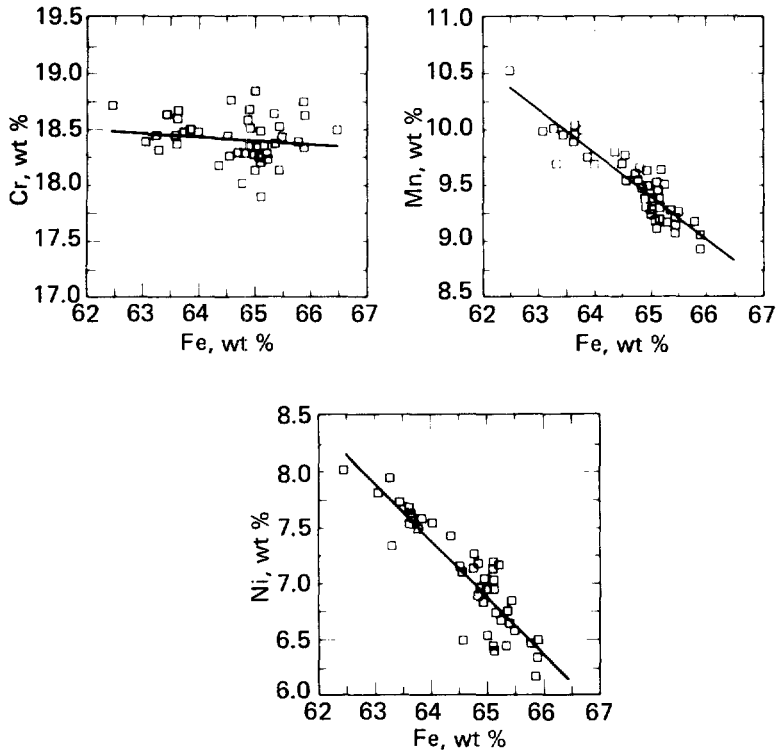

FIG. 3.--Correlations between elemental concentrations in high energy rate forged 21Cr-6Ni-9Mn stainless steel.

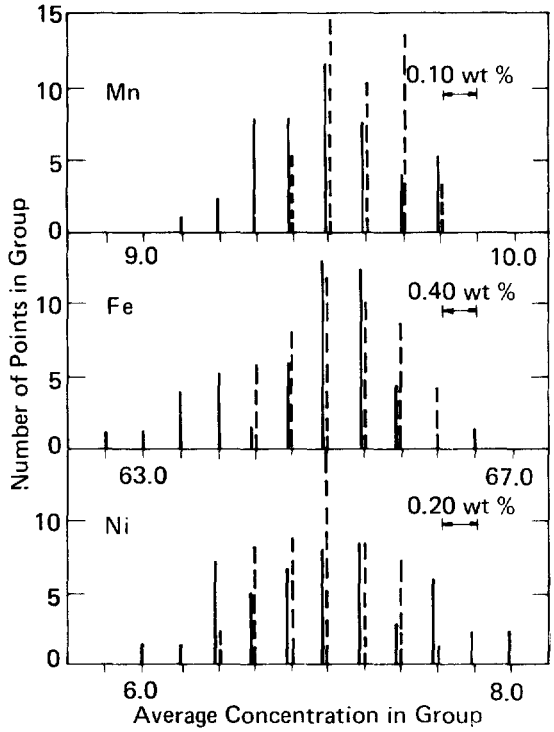

FIG. 4.--Histogram of distributions of elemental concentrations in high energy rate forged (solid bars) and hot cross rolled (dashed bars) 21Cr-6Ni-9Mn stainless steel.

FIG. 5.--High energy rate forged 304L stainless steel.

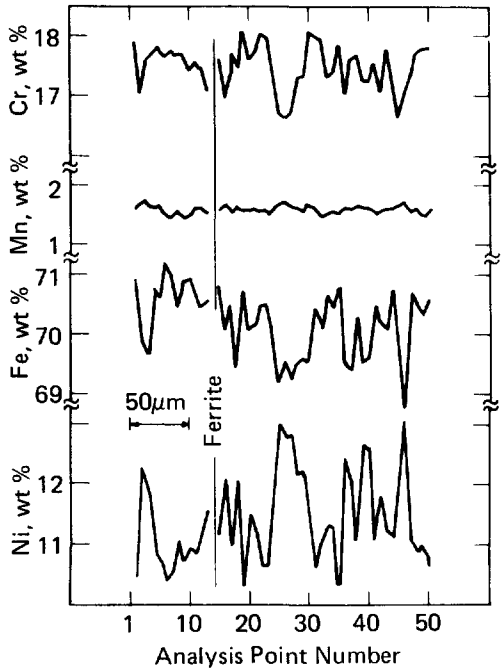

FIG. 6.--Elemental concentration profiles across flow lines in high energy rate forged 304L stainless steel.

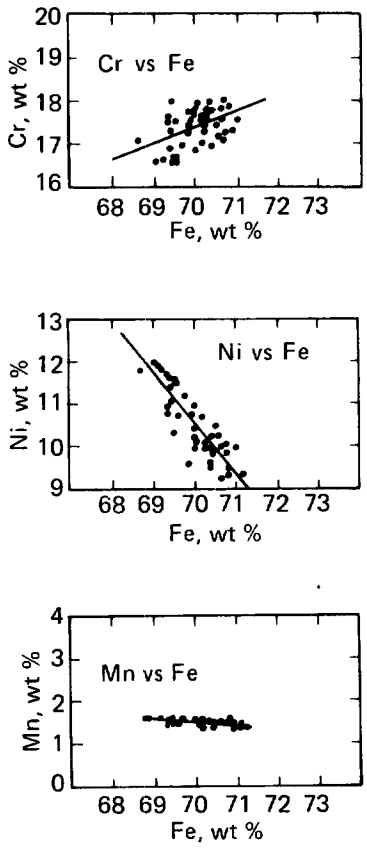

FIG. 7.--Correlation between elemental concentrations in high energy rate forged 304L stainless steel.

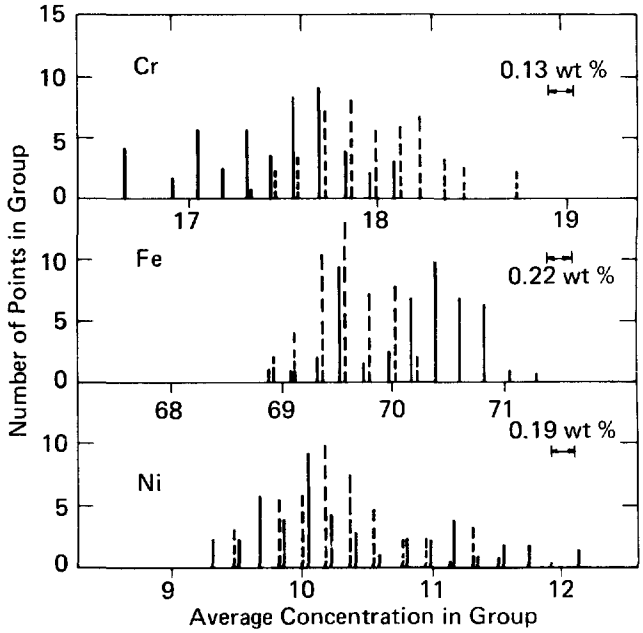

FIG. 8.--Histogram of distributions of elemental concentrations in high energy rate forged (solid bars) and hot cross rolled (dashed bars) 304L stainless steel.

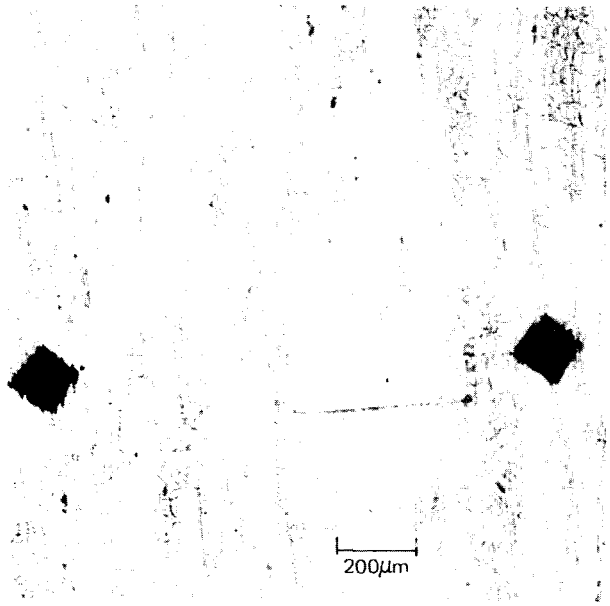

FIG. 9.--Forged 19Ni-18Cr stainless steel.

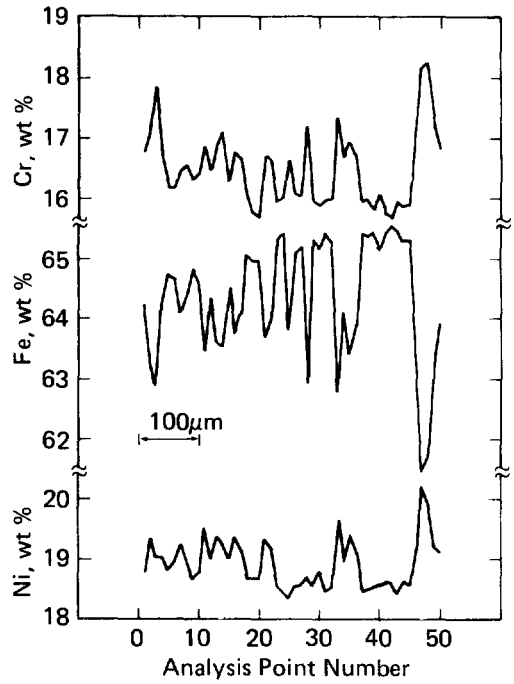

FIG. 10.--Elemental concentration profiles across flow lines in forged 19Ni-18Cr stainless steel.

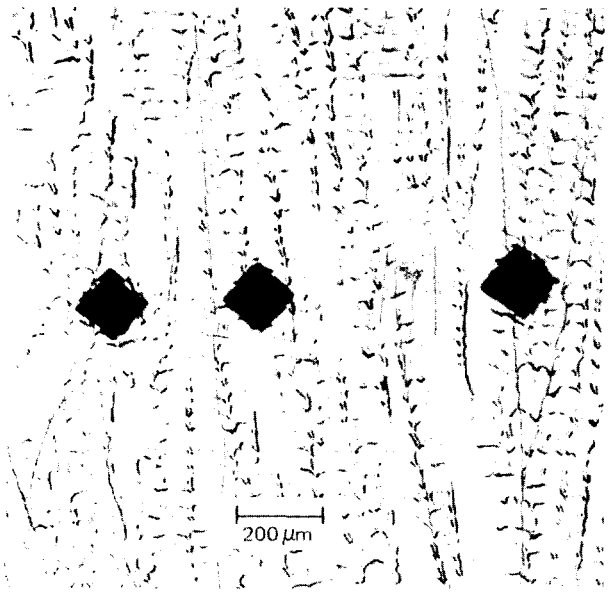

FIG. 11.--Cast 19Ni-18Cr stainless steel.

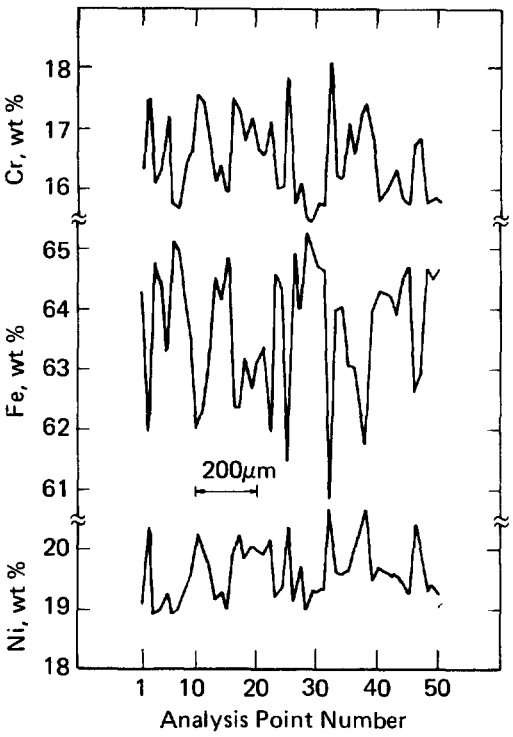

FIG. 12.--Elemental concentration profiles on cast 19Ni-18Cr stainless steel.

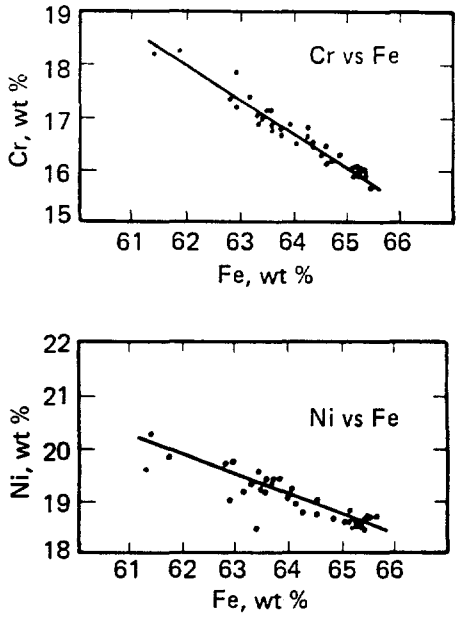

FIG. 13.--Correlation between elemental concentrations in forged 19Ni-18Cr stainless steel.

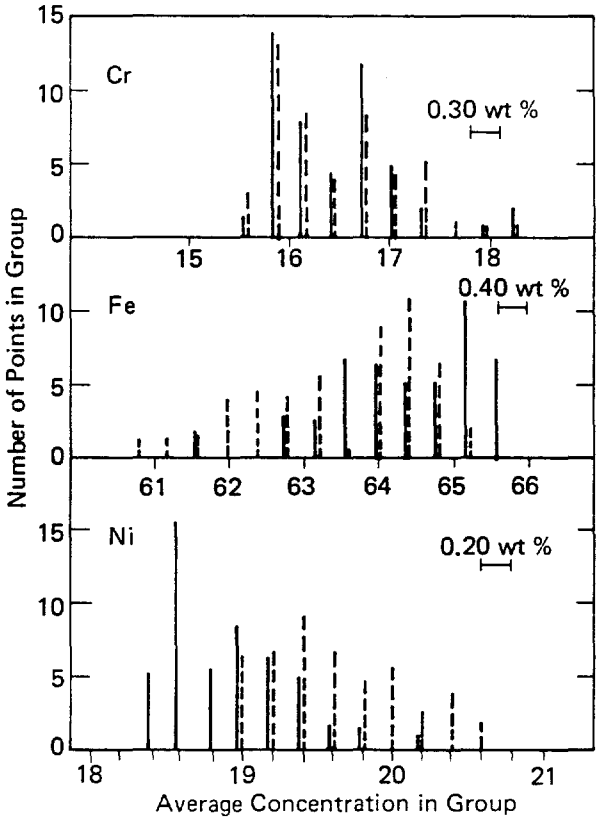

FIG. 14.--Histogram of distributions of elemental concentrations in forged (solid bars) and cast (dashed bars) 19Ni-18Cr stainless steel.